Skarns Associated with the Rize Batholith, North Estern Turkey

ARDESHIR HEZARKHANI[§]

ABSTRACT

According to the mineral compositions, paragenesis, relationships and the fluid inclusion microthermometry two stages of skarn alteration within the Rize pluton area have been identified. The first stage (stage I) was characterized by the Spurrite, vesuviavite, wollastonite, magnetite, pyroxene, gehlenite and garnet assemblages at high temperatures (~750 °C). The second stage (II) occurred at lower temperature (~500 °C) when the system collapsed, and is characterised by tremolite, low temperature vesuvianite, rustumite, epidote, calcite, apatite, titanite and hematite. The vesuvianite displays complex zoning due to fluctuations in the Al^{+3}/Fe^{+3}. The oscillation zones are interpreted to reflect fluid and rock-dominated control of Fe^{+3} and Al^{+3} activities, respectively, and batch-rise or episodic influx of fluid. It is also concluded that the original magma was so poor in metal complexes ($CuCl_2$, $MgCl_2$, $AuCl_2$, ...) to form any economic deposit. The vesuvianite also acts as an index mineral to follow up the geochemical changes within the skarn.

KEYWORD:

Batholite, Skarn, Fluctuation.

1. INTRODUCTION

Emplacement of hydrous magmas at shallow crustal levels leads to the liberation of large volumes of fluid into the surrounding country rocks and, in the case of calcareous rocks, the production of the skarn (Einaudi, 1977). One of the characteristic group minerals crystallizing in higher temperature and low pressure skarns are spurrite, vesuvianite and andradite, and a feature of these minerals is that they commonly display complex, oscillatory zonation (Kwak, and Tan, 1981; Jamtveit et al., 1992). This feature has been interpreted to reflect temporal variations in the composition of the fluid (Crawford, 1977; Kwak and Tan, 1981; Jamtveit, 1991), and thus potentially provides a valuable record of the evolution of the skarn-forming hydrothermal system (Yardley et al., 1991).

In this paper, the nature of major and minor element zonation in vesuvianite and calc-silicates like spurrite, rustumite and gehlenite in skarns associated with the Rize pluton in northeastern Turkey has been documented. These data and information on mineral paragenesis are then used to reconstruct the history of skarn formation and relate the latter to the evolution of the hydrothermal system.

2. GEOLOGICAL SETTING

Turkey is divided into four geotectonic provinces, from north to south; Pontids, Anatolids, Taurids and Border Folds (Ketin, 1966). Granitic rocks occupied wide area of the Pontids and Anatolids provinces. These rocks are formed during the Hercynian and Alpine orogenic movements, and accompany various types of mineralization (Terashima et al., 1988). The Pontids province which is extended east-westward, is geologically subdivided into two different parts; the eastern Pontids, characterized by Cretaceous volcanic and coeval plutonic rocks called Rize plutonic complex (together constituting a volcano-plutonic terrain), and the western Pontids, underlain by Paleozoic sediments and scattered granitic bodies (Terashima et al., 1988).

The Rize batholith is located in the eastern Pontids (Figure 1), in north-western Turkey, and intruded along the Cretaceous volcanic, volcanosedimentary, and carbonate rocks. Rize batholith is a synorogenic (which took place in the main phase during the Laramide tectonic orogeny (Taner, 1979)) and high level composite intrusive consisting of diorite/granodiorite, and andesite dykes (Terashima et al., 1988). Diorite/granodiorite is the most important compositional phase and forms the western part

[§] Department of Mining, Metallurgy and Petroleum Engineering, Amirkabir University of Technology, Hafez Ave., No. 424, Tehran, Iran(e-mail: ardehez@cic.aut.ac.ir).

of the stock at the current erosional level.

The pluton intrudes Upper-Cretaceous volcanoclastic rocks to the north and west and Eocene sediments to the south. Th presence of thermal contact zones defined by spurrite, wollastonite, gehlenite, garnet, and rustumite in

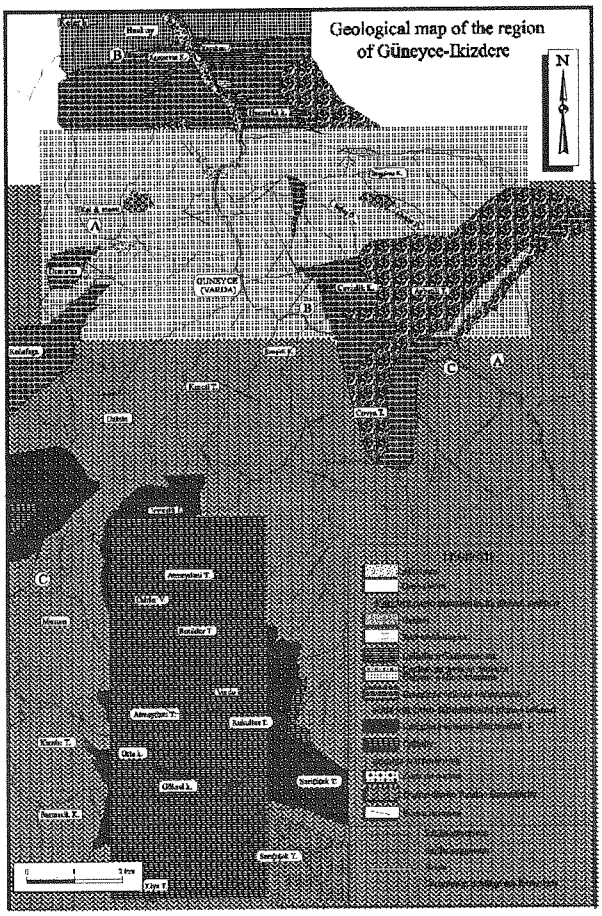

Figure 1: The geological map of Rize batholith area (modified after Taner, 1977).

the country rock indicates a magmatic origin for the pluton (Taner et al., 1979). The minerals examined in this study were sampled from skarns located on the top and eastern margin of the Rize batholith.

3. THE RIZE PLUTON

The oldest rocks exposed in the study area are sequences of Cretaceous volcanic, volcanoclastic (tuff), and limestone with intercalation of shale. The volcanics are calc-alkaline and tuffaceous rocks intruded by numerous calc-alkaline dykes. The Rize batholith which intruded the above rocks during the Alpine orogeny (~40 ma) (Çogulu 1970), has an ellipsoid shape with its main axis oriented SW-NE. It is about 125 km long and 50 km wide (Taner et al., 1979).

4. PETROGRAPHY

Rize diorite/granodiorite is light grey in colour and contains megacrysts of K-feldspar, plagioclase and quartz in a grained matrix. The rock texture ranges from fine-grained in the southern part to coarse-grained in the north and north-east. Almost all the intrusive unit contains the same assemblage of minerals: plagioclase, K-feldspar, quartz, biotite and hornblende (which typically altered to biotite and/or chlorite). The intrusive is generally unfoliated and commonly granular, suggesting a deep level of emplacement (Carten, 1986). The latter interpretation is supported by a quartz hosted fluid inclusion pressure correction, which shows that the maximum depth of intrusion was approximately 2000 to 3000 m (500 to 800 bars).

Phenocrysts comprise about 70 percent by volume of the rock. Mainly zoned plagioclase, zoned K-feldspar, amphibole, quartz and biotite represent phenocrysts. Plagioclase is up to 20 mm in diameter (~30 vol %), K-feldspar is up to 30 mm in diameter (~20 vol %), amphibole is up to 5 mm in diameter (~7 vol %), quartz is up to 17 mm in diameter (~10 vol %), and biotite is up to 4 mm in diameter (<5 vol %). Zoned K-feldspar and zoned plagioclase are crystallized together (subsulvus crsytallization). Amphibole is colorless in normal light, so it could be very low in Fe. Two types of amphibole have been identified in the rock, in the matrix and in the quartz veinlets. Amphibole in the veinlets is less altered than those are in the matrix. The amphibole in the matrix has been replaced by biotite and is only recognizable from the characteristic amphibole morphology of psodomorphs and in some cases rutile needles alligned in the direction of the principal cleavages.

Most of the plagioclase has been altered to sericite, quartz, calcite, and gypsum. Based on the petrography two generations of plagioclase are distinguishable in terms of size, inclusions, and composition; large crystals with altered cores and relatively small crystals with clear Carlsbad twinning (An_{1-5}), that are interpreted to have formed during a later stage of hydrothermal alteration episode. Plagioclase crystals range in composition from oligoclase-andesine in the core (An_{15-35}) to albite (An_{5-15}) at the rim. K-feldspar crystals are altered to clay minerals. They commonly contain small inclusions of primary biotite, plagioclase, and the accessory minerals, apatite, titanite, and zircon. Textural relationships show that plagioclase and K-feldspar crystals formed shortly after amphibole, and that quartz and biotite crystals formed during the last stage of magma crystallization.

The biotite crystals are Pale-brown to greenish-brown, Fe enriched and subhedral. Quartz crystals are anhedral, sometimes rounded, and rarely contain biotite inclusions. The contact between the quartz grains is serrated, forms after high pressure, and/or crystallization of matrix in the cracks. As mentioned above, quartz crystals in this suite are sometimes rounded, suggesting that pressures fluctuated during crystallization (Whitney, 1989). The presence of hornblende crystals, in the freshest samples of the batholith (i.e. an early liquidus phase) indicates that the granodioritic magma contained >3 wt percent H_2O,

which led to water saturation during early crystallization (Whitney, 1989; Burnham, 1979). The latter could be the reason that the diorite was potentially able to alter the Cretaceous carbonate rocks to skarn at the contact.

Accessory minerals are magnetite, hematite, apatite, zircon, rutile, titanite, ilmenite in order of abundance. These minerals occur both in the silicate phases (i.e., biotite, plagioclase and K-feldspar) and interstitial to them (in the groundmass). Magnetite has rutile exolution lamellas and it is altered to hematite in the crystal edges, close to the fractures.

5. ANALYTICAL METHODS

The major-element compositions of skarn minerals, i.e., spurrite, rustumite, gehlenite, vesuvianite and garnet were determined using wavelength-dispersion spectrometry on a JEOL-8900L electron microprobe. Operating conditions were: acceleration voltage 15 kV, beam current 30 nA, spot size 2 μm, and peak counting time 20 s for the most abundant elements (e.g. Si) and for 20 m for elements with lower concentrations, like heavy REEs (e.g., Yb). Representative compositions of vesuvianite, wollastonite, spurrite, rustumite, and gehlenite are given in Tables 1, 2, 3, 4 and 5, respectively. The concentrations of selected trace elements in these minerals were also analysed using a beam current of 80 nA, with peak counting times of 3 minutes. Two type analyses were performed on the mineral samples, microprobe line analyses (traverses), and randomly spot analyses.

6. SKARN MINERALOGY

The Cretaceous limestone and marl units have been altered to skarn adjacent to the Rize pluton. The bulk of the Cretaceous limestone unit consists of massive, medium- to coarse-grained, grey to white marble. The Rize skarn formed mainly in the limestone and marble and less commonly in marls, in a 120m wide zone extending 500 m along the eastern flank of the diorite/granodiorite (west of the Karatas Dere), and in narrower discontinuous bodies adjacent to its western contact. Metasomatic effects are evident along faults and fractures. During contact metamorphism, proximal limestone was converted to a spurrite-vesuvianite skarn, and further from the contact was recrystallized to a marble composed of a interlocking calcite grains with trace quartz and chlorite. The marl is green to greenish-grey colour, and contains intercalated limestone and thin beds of altered volcanoclastic rocks. Marl occurs as thick layers in the upper part of the Cretaceous carbonate sequences. These layers overlie the massive limestone units, which are characterized by the presence of Orbitolina (Index fossil for Cretaceous carbonate rocks). Contact metamorphism produced an aureole ~200 m wide that increases in grade from chlorite facies to pyroxene hornfels facies (spurrite-vesuvianite) at the intrusive contact.

The skarns consist typically of Spurrite, grandite garnet, merwinite, vesuvianite, rustumite, gehlenite, hillebrandite, killalaite, monticellite, tilleyite, and trabzonite (Taner et al., 1998) magnetite, pyroxene, amphibole (tremolite/actinolite), wollastonite, calcite, and minor to trace amounts of dolomite, epidote, quartz, apatite, and titanite. Two main skarn types have been identified, I) spurrite-garnet-pyroxene (+high temperature vesuvianite, wollastonite) skarn, and II) epidote-amphibole (+low temperature vesuvianite) skarn. Based on field relationships, the occurrence of spurrit-garnet-pyroxene skarn namely bodies surrounded and crosscut by epidote-amphibole process. Magnetite is mainly occurring in spurrite-garnet-pyroxene zone, and hematite mainly occurs in amphibole-epidote zones. The observed minerals and mineral assemblages are related to the two different stages of skarn alterations. Based on mineral paragenesis, it is suggested that spurrite, high temperature vesuvianite, diopside, monticellite, gehlenite, and wollastonite were crystallized during the first stage of skarn alteration (stage I), epidote, tremolite, trabzonite, hillebrandite, rustumite, tilleyite, killalaite, chlorite and low temperature vesuvianite mainly during the later stage of skarn formation (stage II). The stage II minerals have been formed by the destruction of high temperature minerals in stage I.

A. Vesuvianite

Two types of vesuvianite have been identified. Type I (high temperature vesuvianite), which appears as euhedral crystals, small crystals, (up to 0.5 mm), contains no fluid inclusions but lots of spurrite solid inclusions (Figure . 2 and 3). Type II (low temperature vesuvianite), which appear as big crystals (up to 15 mm), optically zoned (oscillatory zonations) with a lighter core and darker edges, and contains small (<6 ηm) fluid inclusions. Low temperature vesuvianite shows a massive crystallization, and surrounded the others like spurrite and elongated wollastonite crystals. They are always accompanied by diopside and vary in colour from light green to dark brown in hand samples. In thin section, it forms zoned birefringence, subhedral to euhedral, crystals ranging in diameter from a few hundred ηm to 15 mm, full of solid and liquid inclusions. The solid inclusions are mainly the same as the matrix of the rock and showing very random orientation. They are more than 20 percent of the total rock volume, and mostly altered to a series of alteration minerals such as calcite, epidote, sericite, and other low temperature minerals, evident the very late alteration. Close to the contact with the diorite/granodiorite, the grains of the early stage vesuvianite crystal are finer and commonly display evidence of brittle deformation at their margins. Further from the contact with the intrusive, second stage vesuvianite is more abundant and they crystallized together with spurrite both in the veins and matrix of the rock (Figure 3). Epidote and calcite replace

vesuvianite preferentially (in stage II), while spurrite seems to be intact.

In second type vesuvianite, euhedral crystals are also devcloped where faces project into open fractures or where they are in contact with calcite. The zoning in this type is manifested by an alternation of darker and more birefringence layers. Commonly, the cores are dark brown in polarized light, and surrounded by lots of tiny light and dark twinning (Figure . 3). The zoning occurs on two scales, i.e., surrounding the cores there are alternating thicker anisotropic dark-brown or blue, which in turn toward the outer part contain thin anisotropic brownish-blue layers, respectively.

Six representative samples were chosen for major (Si, Al, Fe, Ti, Ca, Mn and Mg), heavy REEs (Yb, Gd and Er) and trace (F, Cl, Zn and Cu) element analyses of vesuvianite (Table 1). Over 33 electron microprobe analyses were conducted on individual crystals, and compositional maps of Ca, Al, Fe and Mg were prepared for an additional 10 grains (in which are not present in this paper).

Fe^{+2} and Fe^{+3} ratios are not determined, but based on analytical totals and mineral stoichiometry, it is likely that most of the iron occurs as Fe^{+3}. Inspection of the X-ray maps indicates that the colour zoning described earlier and that evident on SEM backscatter images is due to changes in the proportion of the Fe and Al elements, i.e., the zoning could be reflected by variations in the proportions of Al and Fe (i.e., Figure 2).

B. Wollastonite

Wollastonite forms crystals in the matrix of spurrite-vesuvianite skarns and consists of randomly oriented, euhedral to subhedral crystals up to 0.5 mm in diameter. Wollastonite is elongated and oriented in the space between other minerals. Hilleberandite is also crystallized with the spurrite and wollastonite. Hilleberandite form needles with the same orientation as wollastonite and seems to be formed as the result of wollastonite and spurrite alteration.

Two representative samples were chosen for major (Si, Al, Fe, Ti, Ca, Mn and Mg), heavy REEs (Yb, Gd and Er) and trace (F, Cl, Zn and Cu) element analyses of wollastonite (Table 2). Over 15 electron microprobe analyses were conducted on individual crystals, and the major oxides are those of Ca and Si.

C. Spurrite

Spurrite varies in colour from light grey to light pink in hand samples. In thin section, it forms birefringence, albite type twinning, subhedral to euhedral, crystals ranging in diameter from a few hundred microns to 20 mm. Close to the contact with the diorite/granodiorite, the grain size is courser and crystals commonly display evidence of brittle deformation at their margins. Further from the contact with the intrusive, spurrite crystallized with coarse-grained vesuvianite both in the veins and matrix of the rock. Spurrite is also crystallized as small massive patches, and in some case look like a radial crystallization, "completely

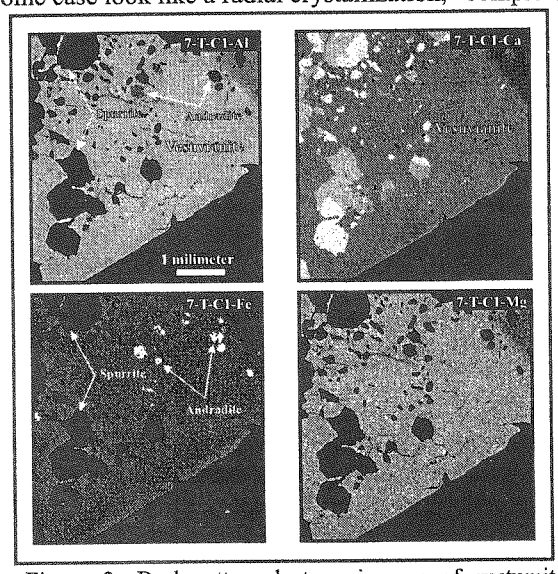

Figure 2: Backscatter electron images of rustumite, spurrite and vesuvianite. The sample numbers are illustrated in the top of each picture separately.

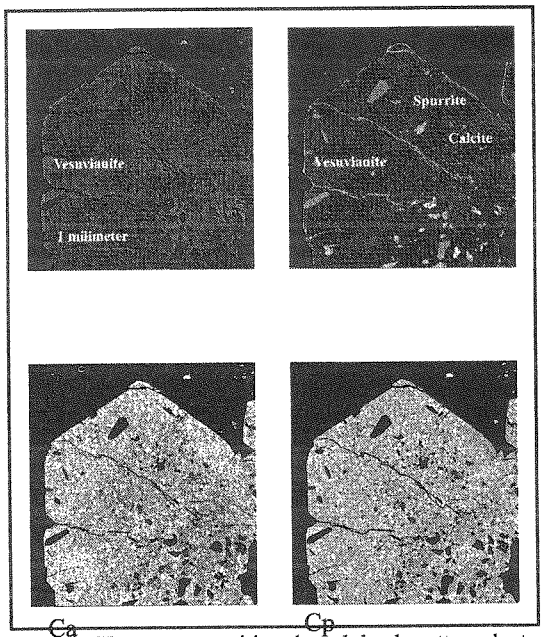

Figure 3: X-ray compositional and backscatter electron images of of vesuvianite from sample no.7-T-C1 from the spurrite-pyroxene zone. Ca = Calcium, Cp = backscattered Image.

circle form". Based on the petrographic observations, it is also evident that both spurrite and calcite crystallized together. Spurrite is full of fractures filled with calcite and smaller spurrite crystals.

Two representative samples of spurrite were chosen for major (Si, Al, Fe, Ti, Ca, Mn and Mg), heavy REEs (Yb, Gd and Er) and trace (F, Cl, Zn and Cu) element analyses (Table 3). Over 28 Electron Microprobe analyses were conducted on individual spurrite crystals. The major oxides are those of Ca and Si. Iron and Mg are in minor concentrations.

D. Rustumite

Rustumite varies in colour from light gray to dark gray in hand samples. In thin section, it forms zoned birefringence, tabular structure, subhedral to anhedral, crystals ranging in diameter from a few hundred microns to 2 mm. Rustumite with the extinction angle of 20 appears as ragged minerals, with high relief and window shape in the calcite and spurrite contact. Euhedral crystals are developed where faces project into open fractures or where they are in contact with vesuvianite. The zoning is manifested by an alternation of thin and darker layers. Commonly, the cores are darker gray in polarized light, and surrounded by tiny light and dark layers.

Two representative samples of rustumite were chosen for major (Si, Al, Fe, Ti, Ca, Mn and Mg), trace (F, Cl, Zn and Cu), and heavy REEs (Yb, Gd and Er) element analyses (Table 4). The major oxides are those of Ca and Si whereas Mg is in minor concentration (Mg ~0.01 atom per formula unit (apfu)).

E. Gehlenite

Gehlenite varies in colour from light to dark grey in hand samples. In thin section, it forms zoned birefringence, subhedral to unhedral, crystals ranging in diameter from a few hundred microns to 1 mm (Figure 2). Close to the contact with the diorite/granodiorite, the grain size is coarser and crystals commonly display fillings. Further from the contact with the intrusive, gehlenite crystallized with more spurrite in the matrix of the rock. Uuhedral crystals are dark and developed where faces project into contact with spurrite (Figure 2).

Two representative samples were chosen for major (Si, Al, Fe, Ti, Ca, Mn and Mg), heavy REEs (Yb, Gd and Er) and trace (F, Cl, Zn and Cu) element analyses of gehlenite (Table 5). Over 17 Electron Microprobe analyses were conducted on crystals.

F. Diopside

Diopside occurs as very ragged, randomly distributed euhedral to subhedral, both, interstitial to spurrite, wollastonite, monticellite and vesuvianite, and as euhedral inclusions in the vesuvianite cores. Diopside appears as dark-brown poikiloblasts (occasionally a few millimetres across) in normal light and with a high relief, elongated and obviously bigger crystals than the epidote crystals. They are also oriented in different directions contain inclusions of magnetite. Diopside is replaced rarely by amphibole (tremolite?) aggregates and calcite during the later stages of alteration.

G. Other skarn minerals

Garnet is crystallized as porphyroblast, surrounding the epidote, and diopside. They are subhedral to unhedral, dark-brown (unisotrope) and highly zoned. Garnet is also both crystallized in the border of the calcite and as small patches between the vesuvianite crystals. Garnets in the border of the calcite contain both solid inclusions (e.g., diopside, graphite, magnetite and rock matrix) and small fluid inclusions (< 3 microns, and not workable for microthermometry analysis). Spurrite is filling the space between the garnet and other minerals like cementing.

Calcite occurs (as a late mineral) both interstitial to the other minerals (e.g., spurrite, vesuvianite, magnetite, hematite and rustumite), and in the veins. Calcite veins cut the vesuvianite crystals very often. In terms of textures, vein-type calcite is subhedral to anhedral and occupied up to 10 percent of the rock volume. Dolomite is obviously smaller than calcite, and is characterized by massive crack filling crystals. Quartz is mainly filling the space between the other minerals as isolated patches. They are full of liquid-rich fluid inclusions. Epidote is also important mineral in the lower temperature skarn altered rocks (stage II). It is granular with the grain size up to 2 mm in diameter and crystallized both in the space of the other minerals and veins (crack fillings). They contain both solid and liquid inclusions.

Magnetite is the most important oxide mineral (up to 1 vol. %) in spurrite-vesuvianite skarn. It occurs as anhedral to euhedral crystals in both the veins and the rock matrix. Traces of magnetite are present in spurrite crystals.

Amphibole (tremolite?) occurs as very small randomly oriented crystals (up to 0.5 mm in long) which replace other minerals (pyroxen) and fill vugs. This suggests a late stage of formation. In vugs, vesuviante and calcite accompany amphibole.

7. ALTERATION STAGES

As mentioned before, based on the mineral paragenesis and field relationships, two stages of alteration have been identified. Stage I represents the peak metamorphic conditions, consists of spurrite, monticellite, calcite, high temperature vesuvianite, diopside, gehlenite, and wollastonite (stage I). At this stage, calcite in carbonate-rich rocks is typically coarse grained (up to 7 mm) and displays polygonal foam textures. The second stage of alteration is characterized by the existence of epidote, tremolite, trabzonite, hillebrandite, rustumite, tilleyite, killalaite, chlorite and low temperature vesuvianite (stage II). Based on mineral paragenesis, it is suggested that, the stage II minerals have been formed by the destruction of high temperature minerals in stage I (Figure 4 and 5). Calcite in the original sediments was replaced by spurrite-pyroxene during stage I skarn alteration, and subsequently wollastonite was formed from remnant calcite. Petrographic observations indicate that calcite was also stable in the stage II alteration, and filled remaining pore spaces. The stability of calcite during stage II alteration could reflect late mixing of high salinity/temperature magmatically derived fluids with lower salinity/temperature meteoric fluids. Decreasing temperature and salinity through mixings can decrease calcite solubility (Ellis, 1963). However, it is not possible to find workable fluid inclusions in calcite to investigate

this hypothesis.

The following reactions show some of the possibilities (due to lack of comprehensive related rock samples) to form early stage minerals (stage I) from the interaction of magmatic fluids and carbonate host rocks:

To form wollastonite;

$$(Cal)\ CaCO_3 + SiO_2 = (Wo)\ CaSiO_3 + CO_2$$

To form grossular garnet;

$$(An)\ CaAl_2Si_2O_8 + (Wo)\ CaSiO_3 + (Cal)\ CaCO_3 = (Grs)\ Ca_3Al_2Si_3O_{12} + CO_2$$

Or,

$$(An)\ CaAl_2Si_2O_8 + 2\ (Cal)\ CaCO_3 + SiO_2 = (Grs)\ Ca_3Al_2Si_3O_{12} + 2\ CO_2$$

To form gehlenite;

$$(An)\ CaAl_2Si_2O_8 + (Cal)\ CaCO_3 = (Gh)\ Ca_2Al_2SiO_7 + (Wo)\ CaSiO_3 + 2\ CO_2$$

Or,

$$2\ (An)\ CaAl_2Si_2O_8 + 3\ (Cal)\ CaCO_3 = (Grs)\ Ca_3Al_2Si_3O_{12} + (Gh)\ Ca_2Al_2SiO_7 + 3\ CO_2$$

To form gehlenite from the early garnet (grossular), it is possible to assume the following reactions:

$$2\ (Grs)\ Ca_3Al_2Si_3O_{12} = (An)\ CaAl_2Si_2O_8 + 3\ (Wo)\ CaSiO_3 + (Gh)\ Ca_2Al_2SiO_7$$

Or,

$$(Cal)\ CaCO_3 + (Grs)\ Ca_3Al_2Si_3O_{12} = (Gh)\ Ca_2Al_2SiO_7 + 2\ (Wo)\ CaSiO_3 + CO_2$$

The following reactions show some of the possibilities to form late stage minerals (stage II) from earlier stage of skarn minerals (stage I):

Alteration of primary wollastonite to tilleyite:

$$(Cal)\ CaCO_3 + (Wo)\ CaSiO_3 = (Til)\ Ca_5Si_2O_8(CO_3)_2 + CO_2$$

Alteration of spurrite to tilleyite:

$$(Spu)\ Ca_5Si_2O_8(CO_3) + CO_2 = (Til)\ Ca_5Si_2O_8(CO_3)_2$$

Alteration of akermanite to tilleyite and monticellite:

$$3\ (Cal)\ CaCO_3 + 2\ (Ak)\ Ca_2MgSi_2O_7 = (Til)\ Ca_5Si_2O_8(CO_3)_2 + 2\ (Mtc)\ CaMgSiO_4 + CO_2$$

To form the smaller and ragged shaped spurrite which seems to be formed latter but still in stage I skarn alteration:

$$3\ (Cal)\ CaCO_3 + 2\ (Ak)\ Ca_2MgSi_2O_7 = (Spu)\ Ca_5Si_2O_8(CO_3) + 2\ (Mtc)\ CaMgSiO_4 + 2\ CO_2$$

And,

$$4\ (Wo)\ CaSiO_3 + (Spu)\ Ca_5Si_2O_8(CO_3) = 3\ (Kil)\ Ca_3Si_2O_7 + CO_2$$

And,

$$4\ (Wo)\ CaSiO_3 + (Spu)\ Ca_5Si_2O_8(CO_3) = 3\ (Kil)\ Ca_3Si_2O_7 + CO_2$$

And,

$$(Til)\ Ca_5Si_2O_8(CO_3)_2 + 4\ (Wo)\ CaSiO_3 = 3\ (Kil)\ Ca_3Si_2O_7 + 2CO_2$$

And,

$$4\ (Mtc)\ CaMgSiO_4 + (Spu)\ Ca_5Si_2O_8(CO_3) + (Kil)\ Ca_3Si_2O_7 = 4\ (Mer)\ Ca_3MgSi_2O_8 + CO_2$$

And,

$$(Spu)\ Ca_5Si_2O_8(CO_3) + 2\ (Mtc)\ CaMgSiO_4 = (Mer)\ Ca_3MgSi_2O_8 + (Cal)\ CaCO_3$$

Or,

$$2\ (Cal)\ CaCO_3 + (Mtc)\ CaMgSiO_4 = (Spu)\ Ca_5Si_2O_8(CO_3) + (Per)\ MgO + CO_2$$

Or,

$$(Cal)\ CaCO_3 + 2\ (Mtc)\ CaMgSiO_4 = (Mer)\ Ca_3MgSi_2O_8 + (Per)\ MgO + CO_2$$

Or,

$$3\ (Cal)\ CaCO_3 + 2\ (Mtc)\ CaMgSiO_4 = (Spu)\ Ca_5Si_2O_8(CO_3) + 2\ (Per)\ MgO + 2\ CO_2$$

And,

$$(Spu)\ Ca_5Si_2O_8(CO_3) + 4\ (Mtc)\ CaMgSiO_4 = 3\ (Mer)\ Ca_3MgSi_2O_8 + (Per)\ MgO + CO_2$$

Or,

$$(Spu)\ Ca_5Si_2O_8(CO_3) + 4\ (Ak)\ Ca_2MgSi_2O_7 = 4\ (Mtc)\ CaMgSiO_4 + 3\ (Kil)\ Ca_3Si_2O_7 + CO_2$$

Or,

$$(Spu)\ Ca_5Si_2O_8(CO_3) + (Ak)\ Ca_2MgSi_2O_7 + 2\ (Mtc)\ CaMgSiO_4 = 3\ (Mer)\ Ca_3MgSi_2O_8 + CO_2$$

$$(Cal)\ CaCO_3 + (Di)\ CaMgSi_2O_6 = (Mtc)\ CaMgSiO_4 + (Wo)\ CaSiO_3 + CO_2$$

$$(Grs)\ Ca_3Al_2Si_3O_{12} + 7(An)\ CaAl_2Si_2O_8 + (Gh)\ Ca_2Al_2SiO_7 + 3\ H_2O = 6\ (Zo)\ Ca_2Al_3SiO_4Si_2O_7(O,OH)$$

$$(Grs)\ Ca_3Al_2Si_3O_{12} + 2\ H_2O + 5(An)\ CaAl_2Si_2O_8 = 4\ (Zo)\ Ca_2Al_3SiO_4Si_2O_7(O,OH) + SiO_2$$

8. FLUID INCLUSION STUDIES FROM THE RIZE SKARN

Fluid inclusions are abundant in quartz crystals in the Rize pluton. They range in diameter from 1 ηm up to 7 ηm. The majority of inclusions examined during this study had diameters of 4-6 ηm. Most of these fluid inclusions are too small (<3 ηm) to be analyzed microthermometrically. Most of our measurements were conducted on the workable fluid inclusions.

9. FLUID INCLUSION CLASSIFICATION

Fluid inclusions were classified into three main types based on the number, nature, and proportion of phases at room temperature:

LV inclusions consist of liquid + vapor ± solid phases with the liquid phase volumetrically dominant. These fluid inclusions are common in all quartz crystals. Their diameter range from 3 to 7 ηm. Vapor bubbles are variable in size, but constitute less than 25 % of inclusion volumes. The inclusions homogenize to liquid. In a small number of

LV fluid inclusions, a cube of halite (< 1 ηm in diameter) was observed. The distribution and volume of solid phases are irregular, (< 5 % to > 10 %) suggesting that they represent trapped solids rather than daughter minerals.VL inclusions also contain vapor + liquid ± solid phases. Vapor bubbles are variable in size, but in all cases consist of > 70 % of the inclusion volume. These inclusions mainly homogenize to vapor, and rarely to liquid, or by critical behavior. Most VL inclusions contain only vapor + liquid. However, some inclusions contain a single solid phase which is either halite or an unidentified mineral, probably also trapped.

LVH inclusions are multiphase, and consist of liquid + vapor ± halite ± other solids (like hematite). They are very rare and very small (<4 ηm) in size. Vapor bubbles occupy < 25 % of the inclusion by volume.

10. Solid Phases in Fluid Inclusions

Halite was identified in the inclusions by its cubic shape and optical isotropy. The identification can be confirmed by SEM-EDAX analyzes. Hematite was easily identified from its red color, hexagonal shape, extremely high index of refraction and high birefringence.

11. Distribution of Fluid Inclusions Types

The Rize intrusion have undergone repeated episodes of fracturing and healing, with multiple generations of fluid inclusions representing the evolution of hydrothermal fluids and corresponding later alterations.

LV inclusions are found in all quartz crystals, but occur in variable proportions. Most LV inclusions are distributed along healed fractures, and are secondary.

VL inclusions are found in quartz phenocrysts from freshest rocks. Some of these inclusions occur in growth zones, where they are accompanied by LVH fluid inclusions, indicating that at least some of them are primary. VL inclusions are generally elongate and have rounded ends, but some have negative crystal shapes. Some of the VL inclusions have variable liquid-vapor ratios, and may have formed from the necking-down of LVH inclusions or heterogeneous entrapment of liquid and vapor.

LVH inclusions up to 6 μm in diameter are found in all quart crystals, from the deepest part of the intrusion (evident of very coarse crystallize sample) through to the shallow levels. Up to two solid phases have been observed in a single LVH inclusion. The co-existence of LVH inclusions and vapor-rich inclusions with consistent phase ratios in the growth zones of quartz grains suggests a primary origin, and co-existence of two immiscible aqueousfluid

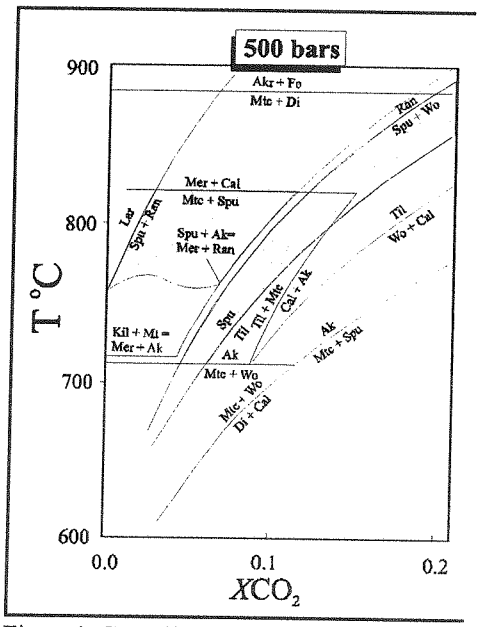

Figure4: Compilation of experimentally determined and calculated T-XCO_2 equilibria at 500 bars in the system CaO-MgO-SiO_2-H_2O-CO_2, showing the stability field of spurrite from Rizeh skarns (modified after Pertsev, 1977).

12. Fluid Inclusion Microthermometry

Microthermometric studies were carried out on 3 samples of quartz from Rize skarns. Temperatures of phase changes in fluid inclusions were measured with a Fluid Inc. U.S.G.S.-type gas-flow stage which operates by passing preheated or precooled N_2 gas around the sample (Werre et al., 1979, Hezarkhani, 2003, 2004). Stage calibration was performed using synthetic fluid inclusions. Accuracy at the standard reference temperatures was ±0.2 °C at -56.6 °C (triple point of CO_2), ±0.1 °C at 0 °C (melting point of ice), ±2 °C at 374.1 °C (critical homogenization of H_2O), and ±9 °C at 573 °C (alpha to beta quartz transition). The heating rate was approximately 1 °C/min near the temperatures of phase transitions.

The temperatures of initial (T_e) and final melting of ice (Tm_{ice}) were measured on types LV, VL and LVH fluid inclusions (Table 6). In the case of type VL inclusions, T_e was difficult to determine, because of the high vapor/liquid ratios. Clathrate formation was not observed in any of the inclusions, which rules out the presence of significant CO_2. The crushing of quartz under anhydrous glycerine confirmed this conclusion; the vapor bubble collapsed during crushing in all but a few inclusions, and

in the latter inclusions the bubble size was unchanged on increased slightly, indicating that the maximum pressure of incondensable gases was ~1 bar.

The temperature of initial ice melting (T_e) of most LV fluid inclusions was between -20 ° and -12 °C, suggesting that NaCl is the principal salt in solution. The Tm_{ice} values for these inclusions range from -1 ° to -7 °C, corresponding to salinities of 1.7 to 9 wt. % NaCl equiv., respectively (Sterner et al., 1988). A small proportion of LV inclusions in quartz phenocrysts from shallow levels have T_e between -19 ° and -35 °C, suggesting the presence of appreciable $CaCl_2$, $FeCl_2$, or $MgCl_2$ in addition to NaCl. The salinity data discussed above ignore a small number of LV inclusions which contain cubes of halite that are interpreted to have been entrapped with the fluid (Table 6).

The T_e value of VL fluid inclusions ranges from -37 ° to -14 °C with a mode of ~-21 °C suggesting that Na is the dominant cations in the solution but that there are significant concentrations of divalent cations. The Tm_{ice} value for these inclusions varies from -0.4 ° to –13.2 °C, which corresponds to salinity between 0.6 and 16.1 wt % NaCl equivalent. The low T_e (-37 ° to -42 °C) for some of the VL inclusions could indicate that these inclusions are the product of necking down of LVH inclusions or heterogeneous entrapment.

A. High temperature phase changes

LV fluid inclusions homogenize to liquid ($Th_{L+V\ L}$) at temperatures between 314 ° and 450 °C, with a well defined mode at Th_L of ~410 °C. Almost all VL inclusions homogenize to vapor ($Th_{V+L\ to\ V}$) between 387 ° and 575 °C.

The liquid and vapor phases in LVH inclusions homogenize to liquid at temperatures between ~230 ° and ~375 °C. Halite in these inclusions is dissolves between 255 °C and 341 °C. Salinities based on the halite dissolution temperature range from 34 to 39.2 wt % NaCl equivalent (Sterner et al., 1988) with an average of 36 wt. % NaCl equivalent. Some of these inclusions did not homogenized on heating to temperatures in excess of 600 °C (limited temperature for the U.S.G.S. equipment).

B. Low temperature phase changes

The temperature of initial ice melting (T_e) of most LV fluid inclusions was between –24.3 ° and –15.3 °C, suggesting that NaCl ± KCl are the principal salts in solution. The Tm_{ice} values for these inclusions range from –2.4 ° to –11.8 °C, corresponding to salinities of 3.6 to 15.9 wt. % NaCl equiv., respectively (Sterner et al., 1988, Hezarkhani, 2004). These fluid inclusions are in the quartz phenocrysts.

The T_e value of VL fluid inclusions ranges from –41.9 ° to –18.1 °C with a mode of ~-26.9 °C suggesting that Na and K are the dominant cations in the solution but that there are significant concentrations of divalent cations. The Tm_{ice} value for these inclusions varies from -0.4 ° to –12.1 °C, which corresponds to salinity between 1.1 and 15.7 wt % NaCl equivalent. The low T_e (dawn to –41.6 °C) for some of the VL inclusions could indicate that these inclusions are the product of necking down of LVH inclusions or heterogeneous entrapment.

13. DISCUSSION

Based on fluid inclusion studies in the Rize hydrothermal system, it is concluded that maximum temperature of ~540 °C and the pressure of 500 to 800 bars, estimated from fluid inclusions could be the P-T conditions for stage II Rize skarn. The temperature for stage I skarn alteration is definitely higher than that for stage II, but due to lack of both suitable equipment and workable fluid inclusions in high temperature phase like spurrite, high vesuvianite, it is not possible to investigate about that at the present time.

During early infiltration of magmatic hydrothermal fluids into the Cretaceous marl and limestone, the original mineralogy of the rock was completely replaced by a calc-silicate assemblage. This assemblage consists of spurrite, rustumite, vesuvianite, garnet, wollastonite, gehlenite, magnetite and diopside.

Spurrite commonly consists of near-end-member. Vesuvianite has grown on a small and resorbed iron-poor core. Microprobe analyses show that Mn and Ti are present in trace amounts in many vesuvianite crystals. Compositional traverses across the vesuvianite indicate that there is no major change in major elements from the core toward the rim of the interest crystals. It suggests a constant equilibrium between the rock and hydrothermal fluid flux during the skarn alteration in Rize skarn system.

Several authors have discussed the permeability generated by skarn alteration. For example, it can be produced by simple fracturing (Einaudi, 1977; Kwak, 1978b; Einaudi, et al., 1982), by chemical reactions between fluids and host rocks (Taylor, 1974), or by a combination of both fracturing and chemical reactions (Kwak and Tan 1981). Petrographic observations and field relationships suggest that for the Rize skarns, a combination of fracturing and chemical reactions created permeability in the Cretaceous carbonate rocks. This is evident from vug formation during the first incursion of hydrothermal fluids into the carbonate rocks (which were the filled by spurrite, vesuvianite, calcite and garnet), and later fracture filling with more calcite, amphibole and epidote. It seems that most of these open spaces were formed by fracturing the system, and not by simple dissolution.

The fluctuation in Al and Fe in zoned vesuvianite is interpreted to reflect changes in the fluid/rock ratio as a result of the episodic infiltration of Fe-rich magmatic fluid interacting with aluminium-rich Cretaceous marls.

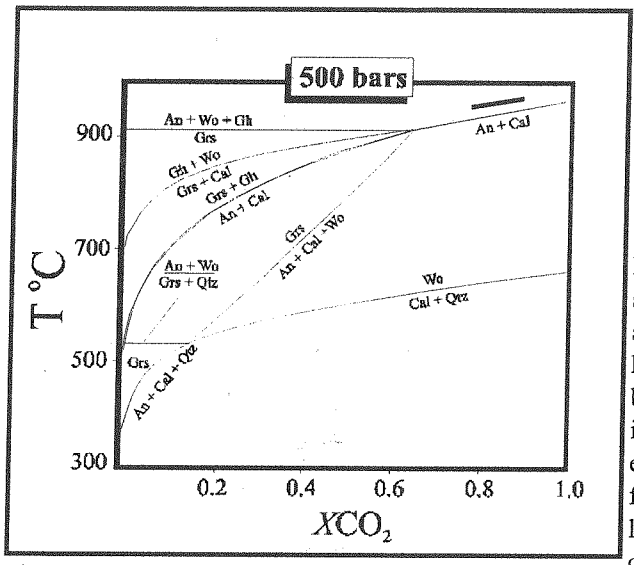

Figure 5: T-XCO_2 diagram at 500 bars for the system $CaO-Al_2O_3-SiO_2-H_2O-CO_2$ calculated using the computer program PTX, Geo-Calc. Pressure of 500 bars is calculated based on the fluid inclusion microthrmometry of the quartz hosted fluid inclusions in the Rize pluton. The temperature is much higher than that was estimated based on the homogenization temperatures of the fluid inclusions from the pluton. The figure is showing the stability field of gehlenite (Brown et al., 1988). The assemblages shown in the diagram are based on the mineralogy of the stage I and stage II key mineral stabilities in Rize skarns. Abbreviations are the same as those in the reaction stoichiometry in the text.

When the fluid/rock ratio was high, the system was fluid buffered and the resulting Fe/Al+Fe ratio was also high due to the Fe-rich nature of the fluid. This caused crystallization of Fe-rich vesuvianite. By contrast, when there was a low fluid influx, the composition of the system was buffered by rock (marls), and the Fe/Al+Fe ratio decreased as a result of the supply of Al from the marl. This caused relatively Al-rich vesuvianite (relatively) crystallization. The only oxide mineral precipitated in this stage was trace magnetite. During stage II alteration increased permeability due to fracturing, faulting, and incursion of hydrothermal fluids caused the system become buffered by the fluid. This could be evident by the formation of amphibole (tremolite), epidote, calcite, quartz, apatite, and titanite.

The replacement of magnetite to hematite in stage II suggests an increasing the fO_2 conditions due to meteoric water flux. Further from the intrusive contact, magnetite is less stable and was replaced completely by hematite, suggesting lower temperatures and possible increasing more meteoric water influence.

Reaction between tremolite-actinolite and diopside suggests that amphibole replaced pyroxene in stage II alteration. In the case of vug and vein fillings, amphibole occurs with quartz and calcite. Quartz occurs interstitial to garnet, amphibole (tremolite) and epidote, which suggest a late origin.

14. CONCLUSIONS

The Rize diorite/granodiorite batholith intruded Cretaceous marl and limestone at approximately Miocene, and produced skarn alteration assemblage. Two stages of hydrothermal activity have been identified. In the first stage, alteration produced spurrite, garnet-pyroxene skarn as a result of reaction of magmatic fluids with the rocks at high temperature (<700 °C) and a pressure of 500 to 800 bars. Oscillatory zonation of vesuvianite reflects variation in Fe/Al ratios, and suggests that fluid/rock ratios varied episodically. At high fluid/rock ratios the system was fluid-buffered and Al-rich vesuvianite crystallized. At lower fluid/rock ratios the rock was able to partially control vesuvianite composition, enabling Fe-rich vesuvianite to crystallize. During this stage, spurrite, magnetite, and pyroxene (diopside) crystallization accompanied vesuvianite crystallization. The pyroxene is diopsidic, suggesting that fO_2 was relatively high (i.e., that the system had a relatively high Fe^{3+}/Fe^{2+}).

The second stage of skarn alteration was marked by the formation of hydrosilicates like tremolite-epidote. Epidote and amphibole precipitation was coincident with the last crystallization of the outer most zones in low temperature vesuvianite, and were accompanied by quartz and calcite. The fluid responsible for this stage alteration was at a lower temperature (~400 °C), and circulated when the hydrothermal system was near collapse. There is no economic mineralization during the both alteration episodes. The author suggests more research activities to find probable REE elements within the skarn.

15. REFERENCES

[1] Crawford, M. L., 1977, Calcium zoning in almandine garnet, Wissahickon formation, Philadelphia, Pennsylvania: CANADIAN MINERALOGIST, v. 15, p. 243-249.

[2] Einaudi, M. T., 1977, Petrogenesis of the copper-bearing skarn at the Mason Valley mine, Yerington district, Nevada: ECONOMIC GEOLOGY, v. 72, p. 769-795.

[3] Einaudi, M. T., and Burt, D. M., 1982, A special issue devoted to skarn deposits, introduction terminology, classification, and composition of skarn deposits, ECONOMIC GEOLOGY, v. 77, p. 745-753.

[4] Einaudi, M. T., Meinert, L. D., and Newberry, R. J., 1982, Skarn deposits, ECONOMIC GEOLOGY, 75th Anniversary,v. 77, p. 317-391.

[5] Ellis, A. J., 1963, The solubility of calcite in sodium chlorite solutions at high temperatures: AMERICAN JORNAL OF SCIENCES. v. 261, p. 259-267.

[6] Harris, N. B., and Einaudi, M. T., 1982, Skarn deposits in the Yerington district, Nevada: Metasomatic skarn evolution near Ludwig, ECONOMIC GEOLOGY, v. 77, p. 877-898.

[7] Hezarkhani, A., (2004), Hydrothermal Evolution in the Raigan Porphyry Copper System Based on Fluid Inclusion studies, (Kerman, Iran): The Path to an Uneconomic Deposit. Amirkabir Journal of Science and Technology, v. 15, No. 57-D, (Basic Science and Applied Engineering), Winter 2004, p. 74-84.

[8] Hezarkhani, A., (2004), Anjerd Skarn Geochemistry and its Association with Economic Copper Mineralization,

Azarbaijan-Iran. Amirkabir Journal of Science and Technology, v. 15, No. 57-D, (Basic Science and Applied Engineering), Winter 2004, p. 158-175.

[9] Hezarkhani, A., (2003), Introducing the Specific Physico-Chemical Conditions in "450 oC" as preventors to Chalcopyrite Deposition in the Sungun Porphyry Copper Deposit, Iran, Amirkabir Journal of Science and Technology, v. 14, No. 55, Summer 2003, p. 865-877.

[10] Jamtveit, B, 1991, Oscillatory zonation patterns in hydrothermal grossular-andradite garnet: non-linear dynamics in regions of immiscibility. AMERICAN MINERALOGIST, v. 76, p. 1319-1327.

[11] Jamtveit, B., Bucher-Nurminen, K., and Stijfhoorn, D. E., 1992, Contact metamorphism of layered shale-carbonate sequence in the Oslo Rift: I. Buffering, infiltration and the mechanisms of mass transport: JOURNAL OF PETROLOGY, v. 33, p. 327-422.

[12] Kwak, T. A. P., and Tan, T. H., 1981, The geochemistry of zoning in skarn minerals at the King Island (Dolphin) Mine: ECONOMIC GEOLOGY, v. 76, p. 468-497.

[13] Pertsev, N. N., 1977, Bisokotemperaturnii metamorphism I metasomatism carbonatnik porod (high temperature metamorphism and metasomatism of carbonate rocks [in Russia]). Akademia Nauk, Moscow, 256 p.

[14] Terashima, S., Taner, M., Yajima, J., and Ishihara, S., 1988, Geochemistry of the Pontids granitoids in Turkey. Bull. Surv. Japan. Vol. 39 (4), p. 251-268.

[15] Taner, M., F., Delayoye, and Vuagnat, M., 1979, On the geochronology by K-Ar method of the Rize pluton the region of Guneyce-Ikizdere, Eastern pontids, Turkey. Schweiz. Mineral, Petrogr. Mitt. 59, 309-317.

[16] Taner, M., 1977, Etude geologique et petrographique de la region de Guneyce-Ikizder, situee au sud de Rize (Pontides orientales, Turquie), Ph.D. thesis, no 1788, 180p.

[17] Taylor, JR. H. P., 1974, The application of oxygen and hydrogen isotope studies to problems of hydrothermal alteration and ore deposition: ECONOMIC GEOLOGY, v. 69, p. 843 883.

[18] Yardley, B. W. D., Rochelle, C. A., Barnicoat, A. C., and Lloyd, G. E., 1991, Oscillatory zoning in metamorphic minerals: an indicator of infiltration metasomatism: MINERALOGICAL MAGAZINE, v. 55, p. 357-365.